Volume 10:1-10

UJEMI+

The Undergraduate Journal of Experimental Microbiology & Immunology (+Peer Reviewed)

Chaperone DegP Is Not Necessary for the Polyhistidine Tag-Detected Secretion of Autotransporter BrkA in *Escherichia coli* BW25113

Loujain Bilal, Ayesha Lalani, Màiri MacAulay, and Parvin Malhi

Department of Microbiology and Immunology, University of British Columbia, Vancouver, British Columbia, Canada

SUMMARY Autotransporters are virulence-associated proteins capable of independent secretion, present on the outer membranes of Gram-negative bacteria. *Bordetella pertussis* is the causative agent of whooping cough and expresses the 103 kDa type Va autotransporter Bordetella resistance to killing (BrkA), which contributes to the bacterium's resistance against the bactericidal activity of the complement pathway. The exact folding mechanisms, including the role of periplasmic chaperones involved in the translocation of BrkA, are not well understood. DegP is a highly conserved periplasmic chaperone that has been implicated in the folding and secretion of other autotransporters in *Escherichia coli* but has yet to be characterized in the expression of BrkA. We therefore hypothesized that DegP would be necessary for BrkA secretion. To investigate this, a 6x histidine tag was inserted in the unstructured region of the BrkA passenger domain for detection by immunoblot analysis. We compared the expression between WT BW25113 and mutant JW0157 (Δ*degP*) cells and observed BrkA surface expression in both conditions, indicating that DegP is not necessary for BrkA secretion. This study provides insight into the secretion process of the virulence factor BrkA and bacterial membrane transport systems which holds the potential for the development of new clinical interventions and biotechnological applications.

INTRODUCTION

Bacterial secretion mechanisms play a pivotal role in the virulence and pathogenicity of Gram-negative bacteria. Among these, autotransporters represent a family of virulence-associated secreted proteins with the unique ability to independently traverse the membranes of Gram-negative bacteria (1). The functions of autotransporters in bacterial pathogenesis are diverse, encompassing critical roles in adhesion, aggregation, biofilm formation, and invasion (1). Type Va proteins are the simplest of the autotransporters, made up of a single polypeptide sequence (2). The polypeptide includes an N-terminus signal sequence responsible for transport across the inner membrane (IM) and a β-barrel transmembrane domain at the C terminal that facilitates the translocation across the outer membrane (OM) (3). Encoded between the signal sequence and the translocation unit is the passenger domain which is the functional and secreted portion of the autotransporter and a short alpha-helical linker region that connects the passenger to the β-domain (2).

Bordetella resistance to killing (BrkA) is a 103 kDa TypeVa autotransporter found on the OM of *Bordetella pertussis,* the causative agent of whooping cough, that functions to inhibit the bactericidal activity of the complement pathway (4). After being synthesized in the cytoplasm, the precursor protein is directed to the IM by its N-terminal signal peptide (SP) and subsequently transported to the periplasm through the Sec system (3). The SP undergoes cleavage in the periplasm and the polypeptide is released into the periplasm (3). Once at the

Published Online: September 2024

Citation: Bilal, Lalani, MacAulay, Malhi. 2024. Chaperone DegP is not necessary for the polyhistidine tag-detected secretion of autotransporter BrkA in *Escherichia coli* BW25113. UJEMI+ 10:1-10

Editor: Ronja Kothe, University of British Columbia

Address correspondence to: https://jemi.microbiology.ubc.ca/

OM, the 30-kDa C-terminus β-core forms an amphipathic β-barrel and the linker region is thought to form a hairpin-like structure, facilitating the translocation of the passenger domain (3). Despite the 73-kDa β-helical passenger domain being cleaved either by its autoproteolytic mechanism or by endogenous OM proteases, it is not detected in the supernatant, suggesting it remains bound to the cell surface through the β-barrel (5, 6). Although progress has been made in elucidating the secretion mechanisms of the autotransporter BrkA, significant gaps persist in our understanding regarding the potential contribution of accessory periplasmic chaperone proteins to its folding within the periplasm and its subsequent translocation to the external environment (7).

Chaperone proteins, belonging to a diverse family of multidomain proteins, play a vital role in assisting the proper folding, stabilization, and transport of other proteins within the cell (8). DegP is a highly conserved periplasmic protein found in bacteria and homologues have been found in yeast and humans (9). In *Escherichia coli,* DegP functions as a chaperone at low temperatures, and proteolytic activity is observed at higher temperatures (9). Previous experiments have shown that DegP is required for the efficient surface expression and location of the autotransporter protein, IcsA, found in *Shigella flexneri* (9). Furthermore, Ruiz-Perez *et al.* studied the role of DegP in the biogenesis of EspP, a prototype SPATE (Serine Protease Autotransporters of Enterobacteriaceae) protein produced by *E. coli* O157:H7 (7). They observed a significant decrease in the secretion of the EspP passenger in the DegP-deficient mutant (7). They further showed direct protein-protein interaction between DegP and the unfolded EspP passenger domain, thus suggesting that autotransporter translocation may require these accessory factors (7).

In this study, we aimed to investigate the role of the periplasmic chaperone DegP on the secretion and surface expression of the autotransporter BrkA as this continues to be unknown. Specifically, the effects of knocking out the DegP chaperone on the surface expression of BrkA were studied in *E. coli* BW25113 cells and detected by a 6x histidine tag (His-tag) engineered into the gene. We hypothesized that knocking out the chaperone DegP would disrupt the secretion of BrkA given its role in the secretion of autotransporters IcsA and EspP (7, 9). In line with this hypothesis, we expected to see a decreased surface expression of BrkA in *E. coli* mutant JW0157 (Δ*degP*) cells as compared to wild-type (WT) BW25113 cells. As BrkA is a known virulence factor, insight into its secretion process could potentially lead to the development of effective treatments against *B. pertussis*, the causative agent of the respiratory infection whooping cough which is responsible for 20 to 40 million cases and 400,000 deaths worldwide annually (10). In addition, a better understanding of the secretion mechanisms of autotransporters can enable the exploitation of the system of traversing bacterial membranes for clinical and biotechnological advancements.

METHODS AND MATERIALS

Preparation of experimental materials. 100µg/µL ampicillin (amp) stock solution was prepared from ampicillin sodium salt and sterile dH_2O. 100µg/µL kanamycin (kan) stock solution was prepared from kanamycin sulphate powder and sterile dH_2O. Luria Burtani (LB) broth was prepared from NaCl, tryptone, yeast extract, and distilled water following the *American Society for Microbiology* protocol (11). For selective LB broth, 100ng/µL of amp and/or 50ng/µL of kan was added. LB agar, LB agar + amp, LB agar + kan, and LB agar + amp/kan plates were prepared with 100ng/µL of amp and/or 50ng/µL of kan using the *Addgene* protocol (12). pDO6935 from Oliver *et al.* (2003) was isolated from *E. coli* DH5α cells from the University of British Columbia Microbiology Department during a previous project (13). 0.1M $CaCl_2$, 0.1M $CaCl_2$ + 15% glycerol, and chemically competent BW25113 and JW0157 cells were prepared following the *UJEMI methods* protocol (14). JW0157 was chosen as the Δ*degP* mutant cell line due to its availability from the Keio Knockout Collection. Subsequently, BW25113 was chosen because it is the wild type of the knockout strain.

Primer Design for pPALMC1. A previous paper by Sun *et al.* inserted an in-frame His-tag and MCS between Gly59 and Gln60 of BrkA, in the N-terminus of the passenger domain (15). To better balance the annealing temperatures, primers were designed with two amino acid residues upstream of the site used by Sun *et al.*, between Asp57 and Ala58. Custom

primers (Table 1) were obtained from Integrated DNA Technologies (IDT) Inc. each with half of a His-tag for insertion into *brkA* on pDO6935.

TABLE. 1 Primers for Q5® site-directed mutagenesis for creation of pPALMC1. Custom primers each designed with half of the intended His-tag (in bold text) at 5' end for insertion between residues Asp57 and Ala58 of *brkA* on pDO6935. Melting temperatures are based on initially annealing bases (not the His-tag nucleotides).

Gene	Primer Sequence (5'- 3')	GC content	Melting Temperature
brkA	F: **CACCACCAC**GCCGGGCAGGAAGGAG	72%	74°C
	R: **ATGATGATG**GTCCTGCGCATGCGGCG	62%	74°C

Q5® site-directed mutagenesis. From the NEB Q5® site-directed mutagenesis kit (#E0554S), Q5® Hot Start High-Fidelity 2X Master Mix and 25ng/µL pDO6925 were combined with 10uM of forward and reverse primer according to manufacturer's instructions (16). 5% DMSO was added to the mixture due to the high GC content of pDO6935. PCR was performed with an initial denaturation step at 98°C for 30s, followed by 25 cycles of PCR. Denaturation was set to 98°C for 10s, annealing was set to 72°C for 30s, and extension was set to 72°C for 210s. The final extension was set to 72°C for 2 minutes. The PCR product was stained with SYBR™ Safe DNA Gel, run on a 1% agarose gel (100V for 90 minutes), and imaged by ChemiDoc MP Imaging System (Bio-Rad) to check for non-specific primer binding and amplification. The PCR product was combined with Kinase, Ligase, & DpnI (KLD) Reaction Buffer, KLD Enzyme Mix and nuclease-free water according to the manufacturer's instructions and left at room temperature for 5 minutes (16). 1µL of the resulting mixture was transformed into competent *E. coli* DH5α from NEB using the heat-shock method, following the manufacturer's instructions (16). Transformed cells were spread-plated on LB amp plates for selection, and grown overnight at 37°C. Colonies were selected from the Q5-product transformed DH5α cell plate and streaked to grow on three separate plates, A, B and C. Several colonies were selected from each streaked plate and grown overnight in LB amp broth for plasmid isolation.

Plasmid isolation, quantification, and gel electrophoresis. Plasmid isolation was accomplished through alkaline lysis via EZ-10 Spin Column Plasmid DNA Miniprep (17). Quantification of DNA concentration and assessment of DNA purity was done using a NanoDrop™ 2000 Spectrophotometer at a wavelength of 260 nm. Plasmids were then stained with SYBR™ Safe DNA Gel, run on a 1% agarose gel (110V for 45 minutes in 1X TAE buffer), and imaged by ChemiDoc MP Imaging System (Bio-Rad) to check for the correct size of anticipated plasmid (7kb) (Figure S1).

Plasmid sequencing and protein structural modelling. Isolated and quantified plasmids were prepared according to the service provider's instructions and sent for whole plasmid nanopore sequencing at Plasmidosauras (18). The sequence of *brkA* from one of the sequenced plasmids, pPALMC1, was run through AlphaFold2 to produce a predicted structural model of BrkA with the inserted His-tag (19)**.**

Transformation of *E. coli* BW25113 and JW0157 cells (Table 2). Adapted protocol from the Hancock Lab (21). 2µL of pDO6935 or pPALMC1 (25 ng of DNA) was added to 100µL of competent *E. coli* BW25113. This was repeated for 100µL of competent *E. coli* JW0157. Cells were heat shocked in a 42°C water bath for 30 seconds and cooled on ice for 1-2 minutes. 1 mL of pre-warmed LB media was added to the cells, and they were incubated for 1 hour at 37°C on a shaking platform. Transformed cells were spread-plated on LB plates with their respective selective antibiotic(s) and grown overnight at 37°C. Single transformant colonies were picked from plates and grown overnight in LB broth with their respective selective antibiotic(s).

Trypsin accessibility assay and isolation of whole-cell lysates. The trypsin accessibility assay was prepared using a combination of Oliver *et al.* and Maurer *et al.,* and whole-cell lysates were prepared using Laemmli's protocol (13, 22, 23). Overnight cultures of *E. coli*

TABLE. 2 Bacterial strains and plasmids used in the study.

	Characteristics	Source
***E. coli* strains**		
BW25113	WT K-12 cells from Keio collection. No antibiotic resistance.	Horizon Discovery Ltd.
JW0157	*ΔdegP* cells from Keio collection (isogenic to BW25113). Kanamycin resistance.	Horizon Discovery Ltd. and verified by V. Hsiung, N. Kucera, K. Sivanesan, and A. Tavakoli Hedayatpoure (UJEMI manuscript in press, 2024)
DH5α	WT chemically competent cells used for transformation. No antibiotic resistance.	NEB Q5® site-directed mutagenesis kit (#E0554S)
Plasmids		
pDO6935	Expression vector with *brkA*. Ampicillin resistance.	Oliver et. al 2003 (13)
pPALMC1	pDO6935 with 6x histidine tag between Asp57 and Ala58 of *brkA*. Ampicillin resistance.	

BW25113 and JW0157 cells transformed with either pDO6935 or pPALMC1 were normalized to an OD_{600} of 0.413. 1.5 mL of each culture was pelleted by centrifugation (5 minutes, 12,000 rpm). Cell pellets were resuspended in phosphate-buffered saline (PBS) and split into two aliquots. Each aliquot of cells was incubated in the presence of either trypsin (2μL of 10 mg/mL) or PBS control for 10 minutes at 37°C. After incubation, cells were pelleted by centrifugation (3 minutes, 14,000 rpm) and washed three times with PBS to stop digestion. Finally, cells were resuspended in 40μL of 2x Laemmli sample buffer (Bio-Rad) + 5% β-mercaptoethanol (BME). Samples were placed in a heat block (95°C) for 1.5 minutes to lyse cells and dissociate the proteins (22). Whole-cell lysates were briefly centrifuged to remove condensation and stored at -70ºC until ready to use for sodium dodecyl sulphate-polyacrylamide gel electrophoresis (SDS-PAGE).

Immunoblot analysis (Figure S2). Whole-cell lysates were resolved using SDS-PAGE at 200 V for 45 minutes. Frozen lysates were thawed on ice and vortexed for 30 seconds before being loaded (15μL) into Mini-PROTEAN® TGX™ Precast Gel (Bio-Rad). Samples were transferred onto a polyvinylidene fluoride (PVDF) membrane using the Trans-Blot Turbo Transfer Pack (Bio-Rad) per manufacturer instructions (24). The membrane was incubated for 5 minutes with Ponceau stain to visualize protein and verify successful transfer from the gel (Figure S2A). Protocol from Cube Biotech western blot for detecting His-tagged proteins was followed with some slight adaptations (25). Membranes were blocked in a blocking buffer (TBS-T with 5% skim milk powder) for one hour. Membranes were then probed with His-tag monoclonal primary antibody (anti-His-tag-Ab) (Invitrogen) diluted to 1:2500 followed by a horseradish peroxidase goat anti-mouse secondary antibody (Invitrogen) diluted to 1:10000 for one hour each. All incubations and washes were done on a shaking platform at room temperature. Enhanced chemiluminescence was completed using Clarity Max™ Performance ECL western blotting substrates (Bio-Rad) and ChemiDoc MP Imaging System (Bio-Rad). Molecular masses were determined using Kaleidoscope™ pre-stained protein ladder (15 μL) and Precision Plus Protein™ unstained protein standard (10μL) from Bio-Rad.

Growth Curve (Figure S3). Protocol adapted from Rogers *et al.* (20). Overnight cultures of *E. coli* BW25113 and JW0157 cells transformed with either pDO6935 or pPALMC1 were diluted 1:100 in LB broth supplemented with their respective selective antibiotic(s) (Table 2). In replicates of 4, 200μL of each diluted culture and LB broth controls were pipetted into a single well of the 96-well Nunc™ MicroWell™ Black Polystyrene Plate (#237105). The OD_{550} of the samples was read in the BioTek Epoch 2 Microplate Spectrophotometer at 37°C

for 24 hours to allow for the bacterial cells to grow to the stationary phase. The data was analyzed and graphically displayed using Microsoft® Excel (Figure S3).

RESULTS

Generation of pPALMC1 with an in-frame His-tag between residues Asp57 and Ala58 of BrkA. To insert a His-tag into *brkA* on pDO6935 for protein detection, we employed Q5® site-directed mutagenesis using custom primers (Table 1). Q5® site-directed mutagenesis included PCR amplification, followed by a KLD reaction to deplete the methylated parent plasmid, and transformation of the cloned His-tag plasmid into *E. coli* DH5α. The cells were plated and grown overnight at 37°C using ampicillin for selection. Several colonies were selected from the plates and grown overnight at 37°C in LB amp broth. Plasmids were subsequently isolated from these colonies and run on an agarose gel to check for the anticipated size (7kb) before being sent for whole plasmid nanopore sequencing (Figure S1). Full plasmid sequencing indicates that the His-tag had been inserted in-frame at the intended site between Asp57 and Ala58 of *brkA* on pDO6935 (Figure 1A, 1B). AlphaFold2 was used

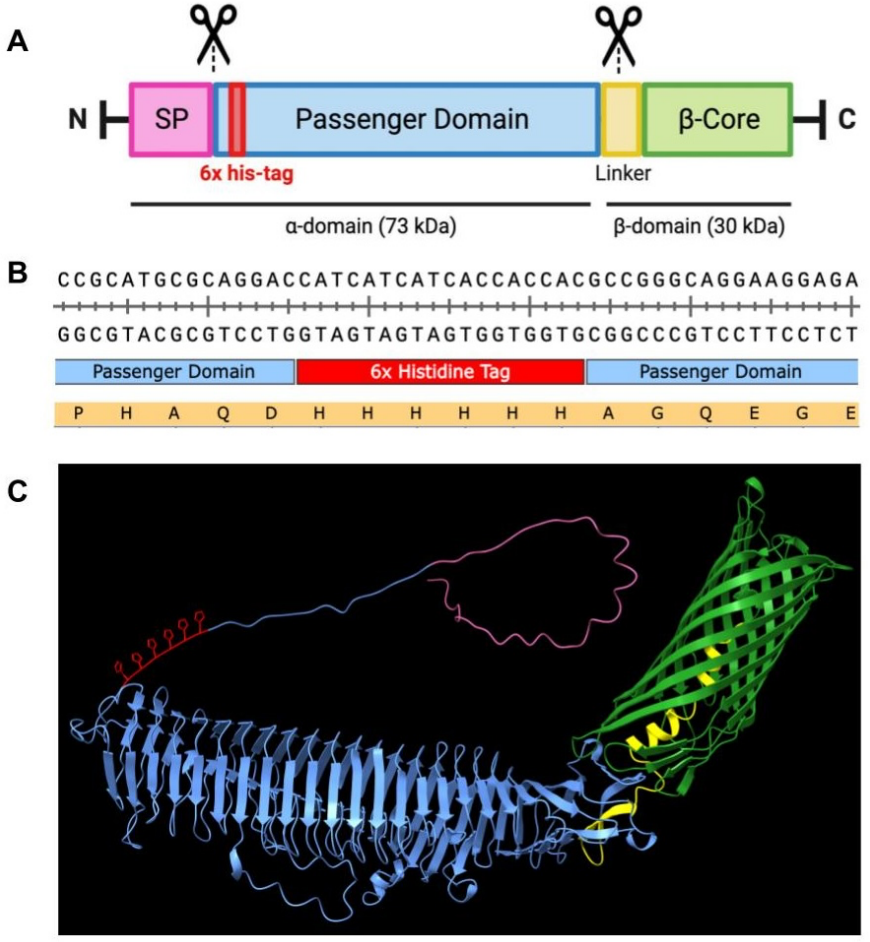

FIG. 1 pPALMC1 has in-frame His-tag between Asp57 and Ala58 in the unstructured region of BrkA passenger domain. (A) Illustrated depiction of BrkA structure showing signal peptide ("SP", pink), passenger domain (blue), His-tag (red), linker region (yellow), and beta core (green), with scissor icons representing cleavage sites. Image is not to scale. (B) Graphical depiction of *brkA* sequence from Pro53 to Gln63 on pPALMC1. (C) AlphaFold2-predicted ribbon structural model of BrkA from pPALMC1 with signal peptide (pink), passenger domain (blue), His-tag with side chains visible (red), linker region (yellow), beta core (green).

to generate a structural model for confirmation that the His-tag was inserted into the unstructured region of BrkA. Insertion into the unstructured N-terminus region of BrkA is ideal as BrkA is secreted via the hairpin model where the C-terminal beta-barrel region forms a pore that the rest of the protein is threaded through, from C-terminal to N-terminal (15). Surface detection of BrkA via the His-tag at that location would therefore indicate whole secretion of the protein. The generated protein structural model shows that the His-tag is in the unstructured region of the passenger domain (Figure 1C) (19). Overall, these results indicate that the generated plasmid, pPALMC1, has an in-frame His-tag inserted between residues Asp57 and Ala58 in the unstructured region of the passenger domain of BrkA.

pPALMC1 transformed *E. coli* BW25113 expresses BrkA on the OM. We first characterized BrkA secretion in *E. coli* BW25113 cells to identify WT secretion. Whole-cell

lysates from BW25113 cells expressing pPALMC1 or pDO6935 (negative control) were isolated and resolved using SDS-PAGE. Protein expression was visualized by western blot using anti-His-tag-Ab and enhanced chemiluminescence (Figure 2). In the BW25113 cells,

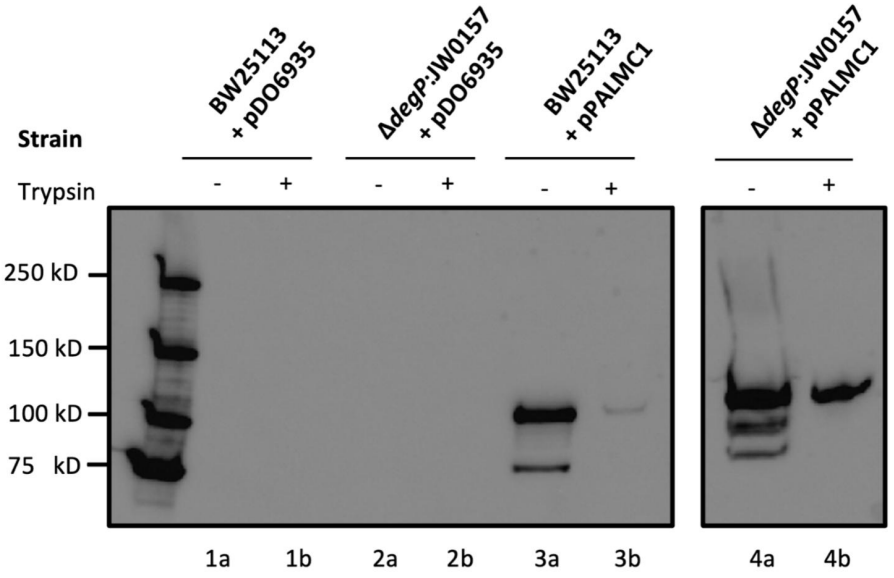

FIG. 2 Western blot analysis of BrkA surface expression in WT and knockout mutant indicates DegP is not necessary for secretion. *E. coli* BW25113 (WT) and mutant JW0157 (Δ*degP*) (mutant) were transformed with either pDO6935 or pPALMC1 and exposed to either trypsin (2 µL of 10 mg/mL) (+) or PBS (-) for 10 minutes at 37°C. OD_{600} was normalized before trypsin assay and whole-cell lysate collection. Immunoblot was performed using a His-tag monoclonal primary antibody (1:2500) and horseradish peroxidase goat anti-mouse secondary antibody (1:10000) to detect His-tagged BrkA. Growth rates of transformed BW25113 and JW0157 cells were similar as seen in Figure S3. Both panels are from the same western blot (Figure S2B) with lanes removed for clarity. Ladder used was Precision Plus Protein™ Standard (Bio-Rad, 10 µL).

two clear bands are seen indicating pPALMC1 expression (Figure 2). A stronger band at approximately 103 kDa is present representing the uncleaved BrkA (Figure 2, lane 3a). It has been observed that the C-terminal of the passenger domain is cleaved at the OM to generate a 73 kDa N-terminal α-domain, thus the lighter band at ~70 kDa represents the cleaved passenger domain (Figure 2, lane 3a) (5). However, after cells were treated with trypsin (2µL of 10 mg/mL) for 10 minutes at 37°C, only a faint band at 103 kDa was seen. Trypsin digests any protein present on the OM including the cleaved passenger domain (73 kDa) and any uncleaved BrkA (103 kDa) that has been secreted. The faint band in the trypsin condition suggests that a greater amount of the BrkA present in the cell is secreted to the membrane (Figure 2, lane 3a) and a smaller amount remains in the periplasm, protected from the protease (Figure 2, lane 3b). BW25113 cells expressing pDO6935 were used as a negative control and no bands were present as the plasmid does not contain a His-tag (Figure 2). Overall, we have demonstrated that the His-tag inserted between Asp57 and Ala58 of the unstructured region of the passenger domain of BrkA does not impede its surface expression (Figure 2, lanes 3a and 3b).

DegP chaperone in *E. coli* is not necessary for BrkA surface expression. To determine the role of the chaperone DegP on BrkA secretion, JW0157 (Δ*degP*) cells were transformed with either pPALMC1 or pDO6935. In JW0157 cells, three bands are present indicating pPALMC1 expression at approximately 103 kDa, 90 kDa, and 73 kDa representing various cleaved forms of BrkA (Figure 2). Similar to the WT expression in lane 3a, the stronger 103 kDa band represents the uncleaved BrkA and the lighter 73 kDa band represents the cleaved N-terminal α-domain (Figure 2, lane 4a). The intensity of the bands suggests that the 103 kDa uncleaved form of BrkA is present at a greater amount compared to the 90 kDa and 73 kDa cleaved segments. By treating JW0157 (Δ*degP*) cells expressing pPALMC1 with trypsin, it was demonstrated that surface expression is occurring in the mutant cells (Figure 2, lane 4b). Only the uncleaved BrkA that remains in the periplasm is protected from trypsin and is represented by the single 103 kDa band (Figure 2, lane 4b). The less intense 103 kDa band and the absence of both the 73 kDa and ~90 kDa cleaved forms of BrkA in the trypsin-treated cells suggests they are accessible to trypsin and therefore, being translocated and expressed on the surface DegP mutant cells. Consequently, the presence of only the 103 kDa in both the WT (Figure 2, lane 3b) and knockout (Figure 2, lane 4b) trypsin-treated lanes suggests the presence of DegP is not necessary for the secretion of BrkA to the OM. Lastly, there are no bands present for the cells expressing pDO6935 (Figure 2, lanes 2a and 2b), functioning as the negative control for the mutant JW0157 (Δ*degP*) cells as the plasmid does not contain a His-tag. Overall, Figure 2 (lanes 4a and 4b) demonstrates that DegP is not necessary for the secretion of BrkA.

DISCUSSION

The objective of this study was to observe whether chaperone DegP is necessary for the secretion of the autotransporter BrkA in *E. coli* BW25113. A His-tag was inserted in the unstructured region of the BrkA passenger domain for detection by immunoblot analysis and we compared expression between WT BW25113 and mutant JW0157 (Δ*degP*) cells.

To detect the expression of BrkA, we used Q5® site-directed mutagenesis to insert a His-tag between residues Asp57 and Ala58 of BrkA. The His-tag was inserted in-frame in the anticipated location in the unstructured region of the BrkA passenger domain (Figure 1). Following the transformation of pPALMC1 into BW25113 WT cells, BrkA was detected by immunoblot analysis using an anti-His-tag-Ab (Figure 2, lanes 3a and 3b). These results indicate that a His-tag inserted at this location in BrkA does not disrupt its secretion. A previous study by Sun *et al.* was similarly able to insert a His-tag, in addition to an MCS, in the unstructured region of the BrkA passenger domain between Gly59 and Gln60 (15). This study did not use the His-tag to detect the full BrkA protein, but instead to detect an exogenous protein cloned into the truncated passenger domain to be expressed using BrkA autotransporter as a display system (15). They used the His-tag to detect expression of the protein on the surface of *E. coli* C41 via immunoblot assay using an anti-His-tag-Ab (15). They therefore demonstrated that a His-tag in the unstructured region of the passenger domain does not disrupt the autotransporter capabilities of BrkA, supporting our findings (15).

Following confirmation of BrkA expression in the BW25113 WT cells (Figure 2, lanes 3a and 3b), pPALMC1 was transformed into mutant JW0157 (Δ*degP*) cells (Figure 2, lanes 4a and 4b). A trypsin accessibility assay followed by cell lysis and immunoblot analysis were performed to determine if BrkA secretion across the outer membrane to the cellular surface was affected in the WT compared to the Δ*degP* mutant. Our results showed that BrkA was cleaved and secreted to the surface in both the WT and mutant (Figure 2). Therefore, DegP is not necessary for protein secretion, which was different from what we hypothesized. Rizzitello *et al*. and Sklar *et al*. demonstrated that a combination of null mutations in *degP, skp* and *surA* resulted in a synthetic phenotype suggesting a functional redundancy in their folding activity which could be explained by parallel pathways (26, 27). They proposed that DepP and Skp are in the same processing pathway and SurA is in a different, but parallel pathway. Hence, the loss of DegP or Skp alone is tolerated by the system through the parallel pathway of SurA, however, losing both pathway components (SurA and DegP) results in a bactericidal phenotype (27). Similarly, Ruiz-Perez *et al.* observed chaperone redundancy where they found overexpression of other chaperone proteins like FkpA and SurA rescued the secretion of autotransporter EspP in a Δ*degP* mutant strain (7). Therefore, the expression of BrkA in both WT and Δ*degP* cells could be explained by the redundancy of DegP with other general periplasmic chaperone proteins suggesting it is not necessary for secretion to the cellular surface.

Interestingly, we observed three bands present in the JW0157 (Δ*degP*) cells at approximately 103 kDa, 90 kDa and 73 kDa with decreasing intensity, respectively (Figure 2, lane 4a). Although 103 kDa and 73 kDa are expected as they represent uncleaved BrkA and the cleaved passenger domain, the 90 kDa was unexpected (6). This unusual 90 kDa band may be explained by similar research conducted by Peterson *et al*. studying the autotransporter EspP in *E. coli* O157:H7 (28). In this study, they observed that by introducing mutations to the C-terminal passenger domain, EspP translocation across the OM is not affected, however, it delayed the secretion of the rest of the passenger domain (28). Using a Proteinase K (PK) accessibility assay, they observed that a large segment of the passenger domain was trapped in the periplasm of ~90 kDa and ~60 kDa (28). Although we saw a differing effect, with our ~90 kDa band presumably present on the cell surface, their findings may explain why it was not only the full uncleaved BrkA (103 kDa) and the cleaved passenger domain (73 kDa) on the cell surface. Considering that DegP is suggested to engage with the C-terminus of its client protein to aid in stabilization and folding, its absence might cause a destabilizing effect on the C-terminus of the BrkA passenger domain (29). The destabilization of the passenger domain C-terminus could affect the speed of translocation through the β-core as according to the hair-pin loop model, the C-terminus is the portion of the passenger domain that is first translocated to the surface (28, 30). Therefore, slower translocation would

result in a portion of the passenger domain remaining trapped in the periplasm causing an unexpected segment of the BrkA protein that is trypsin accessible (i.e. 90 kDa band).

Limitations As this exploratory project was focused on the insertion of a His-tag into pDO6935 and observing the subsequent surface expression of BrkA, a quantitative western blot analysis was not performed. Before the trypsin assay and protein isolation for immunoblot analysis, overnight cultures were normalized to the same OD_{600} to ensure each condition had a similar cell concentration. However, as protein concentration was not normalized, our results are limited by their qualitative nature. Therefore, definitive conclusions cannot be made from the band intensity of the various conditions of the western blot (Figure 2).

Similarly, our findings are also statistically limited as we generated only one viable western blot analysis showcasing pPALMC1 in both the WT BW25113 and mutant JW0157 (Δ*degP*). To accurately investigate and characterize the presence of the third band at 90 kDa in the mutant, replicate western blot assays should be completed.

Lastly, the chaperone DegP is known to have different temperature-dependent functions. At low temperatures (37℃), DegP functions as a chaperone whereas at higher temperatures (42℃) it expresses proteolytic activity (31). As our experiments solely focused on the chaperone role of DegP at 37 ℃, consideration must be taken when extrapolating our findings to the function of DegP in other Gram-negative bacterial hosts, environments, and contexts.

Future Directions Several methods could be employed to address previously mentioned limitations and optimize techniques used in this study. In the future, a Bicinchoninic Acid (BCA) protein assay or similar quantification assay could be used to quantify protein concentration before performing the Western blot to ensure an equal amount of protein is loaded for all samples. This standardization would allow for an accurate quantitative comparison between the level of BrkA surface expression in WT compared to Δ*degP* mutant. Moreover, the presence of the third band at 90 kDa in the JW0157 (Δ*degP*) cells can be further explored and investigated using confirmatory immunoblot analyses.

Furthermore, DegP has been shown to have chaperone activity at lower temperatures while exhibiting proteolytic activity at elevated temperatures when the cell experiences heat stress or when there is an accumulation of misfolded or damaged proteins (31). The temperature-dependent switch between chaperone and protease activities of DegP reflects a sophisticated regulatory mechanism that adapts the cellular response to changing environmental conditions (9). Exploring the impact of BrkA secretion under different temperatures could be another avenue to better characterize the role of DegP in the secretion of the autotransporter BrkA.

Future studies could also investigate the roles of additional chaperone proteins, such as SurA and Skp, to elucidate their contributions to BrkA secretion, as they have been shown to play a role in the secretion of autotransporter EspP (7). The utilization of pPALMC1, constructed in this study, offers a valuable tool for comprehensively understanding BrkA secretion. Ultimately, our investigation into BrkA secretion not only enhances our understanding of fundamental bacterial processes but also holds practical implications for therapeutic development. As BrkA serves as a virulence factor, our findings offer potential avenues for the design of targeted therapeutic strategies against *B. pertussis* and by extension whooping cough, to minimize the impact of the disease on the 20-40 million cases reported annually (4, 10). The elucidation of autotransporter secretion mechanisms in this study contributes to a more comprehensive understanding of bacterial membrane traversal systems, presenting opportunities for advancements in both clinical interventions and biotechnological applications. For example, targeting integral proteins in BrkA's secretion mechanism may be an appealing therapeutic target to protect against *B. pertussis* virulence (4, 15). Furthermore, manipulation of autotransporter secretion systems like BrkA holds biotechnological potential as it can be used to engineer the expression and secretion of proteins of interest on the cell surface for downstream analysis including pathological investigations or drug development (15).

Conclusion Our study investigated whether chaperone DegP is necessary for the surface expression of the autotransporter BrkA. Surface expression in mutant JW0157 (Δ*degP*) and WT BW25113 cells was detected using a non-disruptive His-tag inserted between residues Asp57 and Ala58 in the unstructured region of the passenger domain of BrkA. In contrast to our hypothesis, we found that DegP is not necessary for surface expression of BrkA in *E. coli* as surface expression was observed in both JW0157 (Δ*degP*) cells and BW25113 cells following transformation with pPALMC1 and immunoblot analysis.

ACKNOWLEDGEMENTS

We would like to thank the MICB 471 teaching and laboratory support team, specifically Dr. David Oliver, Charlotte Clayton, and Jade Muileboom, for their support and guidance during this project. We would also like to thank the UBC Department of Microbiology and Immunology for the funding and resources for this project. Finally, we would like to acknowledge V. Hsiung, N. Kucera, K. Sivanesan, and A. Tavakoli Hedayatpoure (UJEMI manuscript in press, 2024) for generously providing and confirming the knockout of the JW0157 Δ*degP* mutant strain. We would also like to thank two anonymous reviewers for constructive feedback on this manuscript.

CONTRIBUTIONS

Co-authorship should be considered equal between Loujain Bilal (LB), Ayesha Lalani (AL), Màiri MacAulay (MM), and Parvin Malhi (PM) for this manuscript. All authors contributed equally to designing the study, completing experimental procedures in the laboratory, and troubleshooting throughout the term. LB contributed to the writing of results, discussion, and limitations as well as the generation of Figure 2 and Supplemental Figures 1 and 2. AL carried out the growth curve, generated its subsequent Figure 3, and contributed to Supplemental Figures 1 and 2 and the writing of the discussion. MM designed the primers used, generated Figure 1 and Tables 1 and 2, and contributed to writing the results and discussion. PM wrote the introduction, conclusion, and future directions. All authors contributed to writing the title, abstract, methods, and references. All authors edited the draft version of the manuscript.

REFERENCES

1. **Wells TJ, Tree JJ, Ulett GC, Schembri MA**. 2007. Autotransporter proteins: novel targets at the bacterial cell surface. *FEMS Microbiol Lett* **274**:163–172.
2. **Fan E, Chauhan N, Udatha DBRKG, Leo JC, Linke D**. 2016. Type V Secretion Systems in Bacteria. *Microbiol Spectr* **4**:10.1128/microbiolspec.vmbf-0009–2015.
3. **Henderson IR, Navarro-Garcia F, Nataro JP**. 1998. The great escape: structure and function of the autotransporter proteins. *Trends Microbiol* **6**:370–378.
4. **Barnes MG, Weiss AA**. 2001. BrkA Protein of *Bordetella pertussis* Inhibits the Classical Pathway of Complement after C1 Deposition. *Infect Immun* **69**:3067–3072.
5. **Oliver DC, Fernandez RC**. 2001. Antibodies to BrkA augment killing of *Bordetella pertussis*. *Vaccine* **20**:235–241.
6. **Oliver DC, Huang G, Nodel E, Pleasance S, Fernandez RC**. 2003. A conserved region within the *Bordetella pertussis* autotransporter BrkA is necessary for folding of its passenger domain. *Mol Microbiol* **47**:1367–1383.
7. **Ruiz-Perez F, Henderson IR, Leyton DL, Rossiter AE, Zhang Y, Nataro JP**. 2009. Roles of Periplasmic Chaperone Proteins in the Biogenesis of Serine Protease Autotransporters of Enterobacteriaceae. *J Bacteriol* **191**:6571–6583.
8. **Saibil H**. 2013. Chaperone machines for protein folding, unfolding and disaggregation. *Nat Rev Mol Cell Biol* **14**:630–642.
9. **Purdy GE, Hong M, Payne SM**. 2002. *Shigella flexneri* DegP Facilitates IcsA Surface Expression and Is Required for Efficient Intercellular Spread. *Infect Immun* **70**:6355–6364.
10. Pertussis (whooping cough). Public Health Agency of Canada. https://www.canada.ca/en/public-health/services/immunization/vaccine-preventable-diseases/pertussis-whooping-cough.html. Retrieved 3 August 2024.
11. **MacWilliams M, Liao M-K**. 2006. Luria Broth (LB) and Luria Agar (LA) Media and Their Use Protocol. American Society For Microbiology.
12. Addgene: Pouring LB Agar Plates. https://www.addgene.org/protocols/pouring-lb-agar-plates/. Retrieved 15 December 2023.
13. **Oliver DC, Huang G, Fernandez RC**. 2003. Identification of Secretion Determinants of the *Bordetella pertussis* BrkA Autotransporter. *J Bacteriol* **185**:489–495.

14. **Chang AY, Chau, Vivien WY., Landas, Julius A., Pang, Yvonne**. 2017. Preparation of calcium competent *Escherichia coli* and heat-shock transformation. *JEMI Methods* **1**:22–25.
15. **Sun F, Pang X, Xie T, Zhai Y, Wang G, Sun F**. 2015. BrkAutoDisplay: functional display of multiple exogenous proteins on the surface of *Escherichia coli* by using BrkA autotransporter. *Microb Cell Factories* **14**:129.
16. 2020. Instruction Manual Q5 Site-Directed Mutagenesis Kit. New England BioLabs Inc.
17. 2019. Bio Basic EZ-10 Spin Column Plasmid DNA Miniprep Kit Product Info Booklet. Bio Basic Inc.
18. **McGuffie MJ, Barrick JE**. 2021. pLannotate: engineered plasmid annotation. *Nucleic Acids Res* **49**:W516–W522.
19. **Jumper J, Evans R, Pritzel A, Green T, Figurnov M, Ronneberger O, Tunyasuvunakool K, Bates R, Žídek A, Potapenko A, Bridgland A, Meyer C, Kohl SAA, Ballard AJ, Cowie A, Romera-Paredes B, Nikolov S, Jain R, Adler J, Back T, Petersen S, Reiman D, Clancy E, Zielinski M, Steinegger M, Pacholska M, Berghammer T, Bodenstein S, Silver D, Vinyals O, Senior AW, Kavukcuoglu K, Kohli P, Hassabis D**. 2021. Highly accurate protein structure prediction with AlphaFold. 7873. *Nature* **596**:583–589.
20. **Rogers A, Bullard K, Dod A, Wang Y**. 2022. Bacterial Growth Curve Measurements with a Multimode Microplate Reader. BIO-Protoc 12.
21. **Hancock REW**. 1999. CaCl2 Transformation of *E. coli.* Hancock Laboratory Methods.
22. **Laemmli UK**. 1970. Cleavage of Structural Proteins during the Assembly of the Head of Bacteriophage T4. 5259. *Nature* **227**:680–685.
23. **Maurer J, Jose J, Meyer TF**. 1997. Autodisplay: one-component system for efficient surface display and release of soluble recombinant proteins from *Escherichia coli*. *J Bacteriol* **179**:794–804.
24. Trans-Blot Turbo Transfer System Transfer Pack Quick Start Guide. Bio-Rad.
25. 2013. Western Blot and chemiluminescent immunodetection of His-tagged proteins. Cube Biotech.
26. **Sklar JG, Wu T, Kahne D, Silhavy TJ**. 2007. Defining the roles of the periplasmic chaperones SurA, Skp, and DegP in *Escherichia coli*. *Genes Dev* **21**:2473–2484.
27. **Rizzitello AE, Harper JR, Silhavy TJ**. 2001. Genetic Evidence for Parallel Pathways of Chaperone Activity in the Periplasm of *Escherichia coli*. *J Bacteriol* **183**:6794–6800.
28. **Peterson JH, Tian P, Ieva R, Dautin N, Bernstein HD**. 2010. Secretion of a bacterial virulence factor is driven by the folding of a C-terminal segment. *Proc Natl Acad Sci* **107**:17739–17744.
29. **Harkness RW, Ripstein ZA, Di Trani JM, Kay LE**. 2023. Flexible Client-Dependent Cages in the Assembly Landscape of the Periplasmic Protease-Chaperone DegP. *J Am Chem Soc* **145**:13015–13026.
30. **Shannon JL, Fernandez RC**. 1999. The C-Terminal Domain of the Bordetella pertussis Autotransporter BrkA Forms a Pore in Lipid Bilayer Membranes. *J Bacteriol* **181**:5838–5842.
31. **Spiess C, Beil A, Ehrmann M**. 1999. A Temperature-Dependent Switch from Chaperone to Protease in a Widely Conserved Heat Shock Protein. *Cell* **97**:339–347.